REMOTE SENSING TO ASSESS REGIONAL CLIMATIC EFFECTS OF URBAN EXPANSION IN NORTHERN BANGKOK, THAILAND

Tran Hung, Yoshifumi Yasuoka

Institute of Industrial Science, University of Tokyo

4-6-1 Komaba, Meguro-ku, Tokyo 153-8505, Japan

Tel: +81-3-5452-6415 Fax: +81-3-5452-6410 E-mail: tranhung@iis.u-tokyo.ac.jp

ABSTRACT: The northern suburb of the Bangkok Metropolis, Thailand has experienced rapid urban expansion at the rate of > 7 percent per year in some areas during the 1985-1993 period. The sub-urbanization brought by human activity has created not only significant socio-economic transformations in the rural surroundings, but also changes in regional environment. In this study, we used satellite images from 1986 through 1999 combined with ancillary data to monitor the land cover changes and to determine the urban development patterns over time. Two TM scenes of 1989 and 1999 were utilized to derive surface biophysical parameters such as fractional vegetation cover (Fr), surface radiant temperature (T_s), surface moisture availability (M_0) and evapotranspiration fraction (ET/Rn) using the so-called “triangle method”. The relationship between those parameters and percentage of urbanized land was, then, examined to reveal significant factors affecting the microclimate changes in response to the urban expansion. The findings from this study could provide urban planners insights into mechanisms of the urban-induced environmental changes due to the rapid expansion of the Bangkok Metropolis.

KEYWORDS: Regional climate, TM images, urbanization, urban planning, Thailand

1. Background

Bangkok, one of fast-growing Asian Metropolis agglomerations with population of more than 10 million, is a primate city of Thailand. As the city expands, prime agricultural land and habitats such as forests and water basins are transformed into land for housing, roads, and industry. Thus, the drastic changes of land cover and land-use caused by urbanization could significantly affect social, economic and ecological conditions in a large urban footprint area. While effective urban land use planning can help guide urban development away from vulnerable ecosystems, it appears impossible without deep understanding of processes governing the change dynamics and their inter-relations in urban and sub-urban areas. It is well recognized that the multi-spectral, multi-temporal satellite imageries provide the most reliable and consistent means of monitoring land cover changes associated with urbanization at the regional scale. Ridd (1995) noted, however, that quantitative biophysical information could also be extracted from existing satellite data, thus adding a great potential for practical application to regional planning and urban ecology. Remotely sensed surface radiant temperatures were successfully used in the studies of the so-called urban heat islands (Nichol, 1996), while various vegetation indexes have long been used in urban vegetation studies. Carlson *et al.* (1990) has discovered the characteristic triangular-shaped envelope of pixels envelope as viewed on a scatterplot of vegetation cover and surface radiant temperature for satellite remotely sensed pixels. Moreover, Gillies *et al.* (1997) demonstrated that regardless of the scale of measurement, the triangular shape is typical for scatterplots made from satellite images of large heterogeneous regions under strong sunlit conditions. This based on the facts that depending on variations on soil moisture, bare ground and partially vegetated surfaces display a large range in surface radiant temperature, which then decreases to the less variable temperature of dense vegetation. The borders of the triangle constrain the solutions for determining the surface energy fluxes and different parts of the triangle correspond to

different types of surfaces. Carlson *et al.* (1990) has developed a Soil-Vegetation-Atmosphere Transfer (SVAT) model to predict changes in various meteorological variables, including substrate temperature, atmospheric temperature and surface moisture as a function of time. The remotely-sensed measured variables in terms of surface radiant temperature and Normalized Difference Vegetation Index (after normalizing to minimize the effects of surface and atmospheric variability) could be then fitted to the model's simulated ones in order to solve the inverse problem of estimating fractional vegetation cover, surface moisture availability and evapotranspiration fraction (Gillies *et al.*, 1997). Owen *et al.* (1998) and Carlson *et al*. (2000) have developed the so-called "triangle method" to derive surface biophysical parameters from AVHRR imageries and to trace out the pixel trajectories over time associated with land cover changes. They have successfully explored various climatic effects of urban development during 9-year periods for Centre and Chester Counties, Pennsylvania, USA.

In this paper, we have applied the "triangle method" to derive surface biophysical parameters such as surface radiant temperature (T_s), surface moisture availability (M_0), evapotranspiration (ET/Rn) fraction and vegetation fraction (Fr) from high-resolution TM images for a tropical region. The rapidly urbanized area of Northern Bangkok Metropolis was chosen as a case study. The integration of remote sensing derived land covers with ancillary information has monitored the surface development over the last two decades and provided insights into socio-economic transformations associated with urbanization in the area. The main objective of this paper is to illustrate the expanded capability of remote sensing in studying the impacts of rapid urbanization on regional environment by analyzing the changes in biophysical parameters associated with urban development in the Northern Suburb of Bangkok Metropolis between 1989 and 1999. The image processing/GIS systems used were

ERDAS Imagine 8.5, ENVI 3.2, ArcView 3.2 and SPSS for Windows 9.0 was used for statistical analysis.

2. Site Description and Data used in Land Use Mapping

Administratively, the study area composes of the Pathum Thani and Nonthaburi province and parts of Northern Bangkok Metropolis, Nakhon Pathom and Ayuthaya provinces (Figure 1). The natural conditions such as flat topography, good alluvium soil and sufficient irrigation system in the heart of the Chao Phraya delta favor the development of intensive agriculture for years in the study area, primarily for irrigated rice crop cultivation. However, with the expansion of Bangkok Metropolitan Administration (BMA), the rice land-use, which has dominated more than 20 years before, has been changed steadily to other land-uses such as urban and industrial areas, fruit tree, vegetables plantation (Figure 2). Due to the relocations of industries from BMA, there was a dramatic increase in industrial establishment in the area (Figure 3a). In 1998, for example, there were 350 new factories creating 221,000 employment opportunities in the Pathum Thani province alone, where the industrial sector took the largest share in GPP. High economic growth and increased employment opportunities caused substantial influx of labor immigration, which accounted up to 200,000 unregistered persons as compared to the 616,000 official population figure in 1998 in the Pathum Thani province alone. The sub-urbanization has speeded up with 52% of urban population in 1990, increased to 61% in 1995 and predicted to reach 82% in 2020. Rapid land-use changes associated with imbalanced growth pattern in the area give rise not only to serious social problems but also create various environmental problems such as air/water pollution, urban heat islands, land subsidence, etc. In addition, the land conversion from irrigated paddy fields (which could serve as local water reservoir during flood) to built-up areas has reported to increase the Chao Phraya river flooding hazards to the Bangkok city.

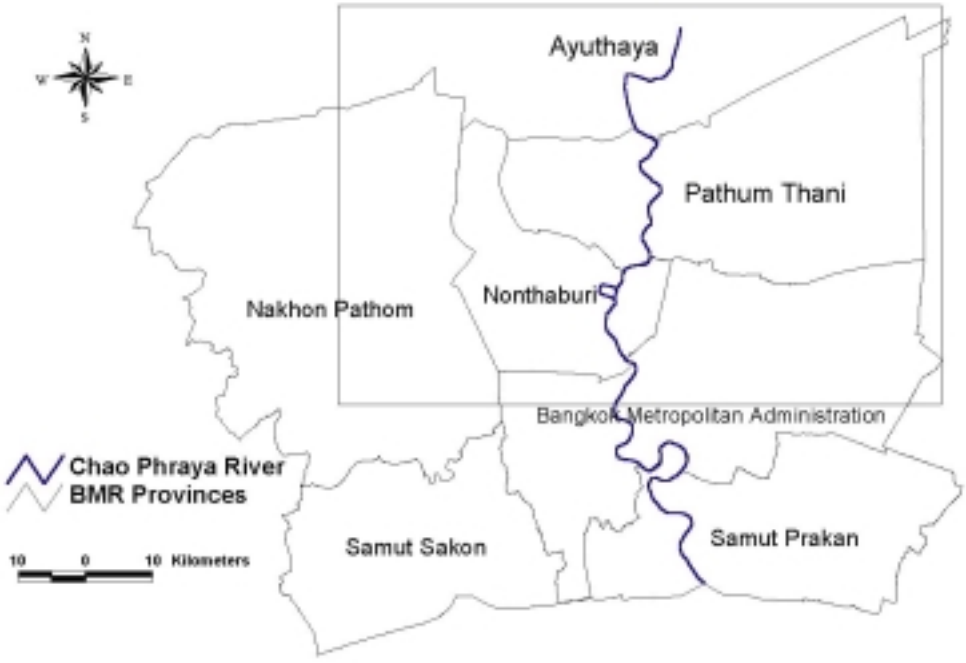

Figure 1 Location of the study area (indicated by the rectangular box) in relation with Bangkok Metropolitan Region (BMR) and the Chao Phraya river.

Satellite images LANDSAT (MSS 1986 and TM 1989, 1990, 1992, 1999) and SPOT 1993 were obtained for the study area to provide temporal land cover and land use information. Dry season scenes were used since there are less cloud covers and thus permit a better distinction between forested, agricultural and urban or built-up land covers. Satellite images were corrected for atmospheric attenuation and geo-referenced to a common 1:50,000 UTM topographic map base. The geo-corrected images were then submitted to image analysis system (ERDAS Imagine) to update road and irrigation networks, stratify scenes into vegetation/non-vegetation areas using NDVI and built-up/non-built-up areas using texture measures. The ancillary data such as existing land use maps and stratified maps were used to improve classification maps in the post-classification procedures. The image analysis had been done on single-date images individually and the change detection was based on post-classification techniques with raster GIS functions involving image co-registration (all images

were re-sampled to 80-m squares with a nearest neighbor interpolation algorithm) and overlaying. The images were classified according to several basic land surface types. Although the classification process was capable of reasonably separating 15-18 land cover classes, given the objectives of the study and real situations of the area, the final analysis consolidated these into 7 land-cover categories: built-up, paddy, fruit-tree plantation, water-body, fallow land and unclassified vegetation (horticulture, coconut, palm trees, etc.) with assistance of existing land-use maps. The aggregating into more broad land-use categories has also increased significantly the accuracy of image classification, making classified images more comparable with existing land use maps. The details of image analysis procedures used in land use mapping could be found in Tran & Yasuoka (2000).

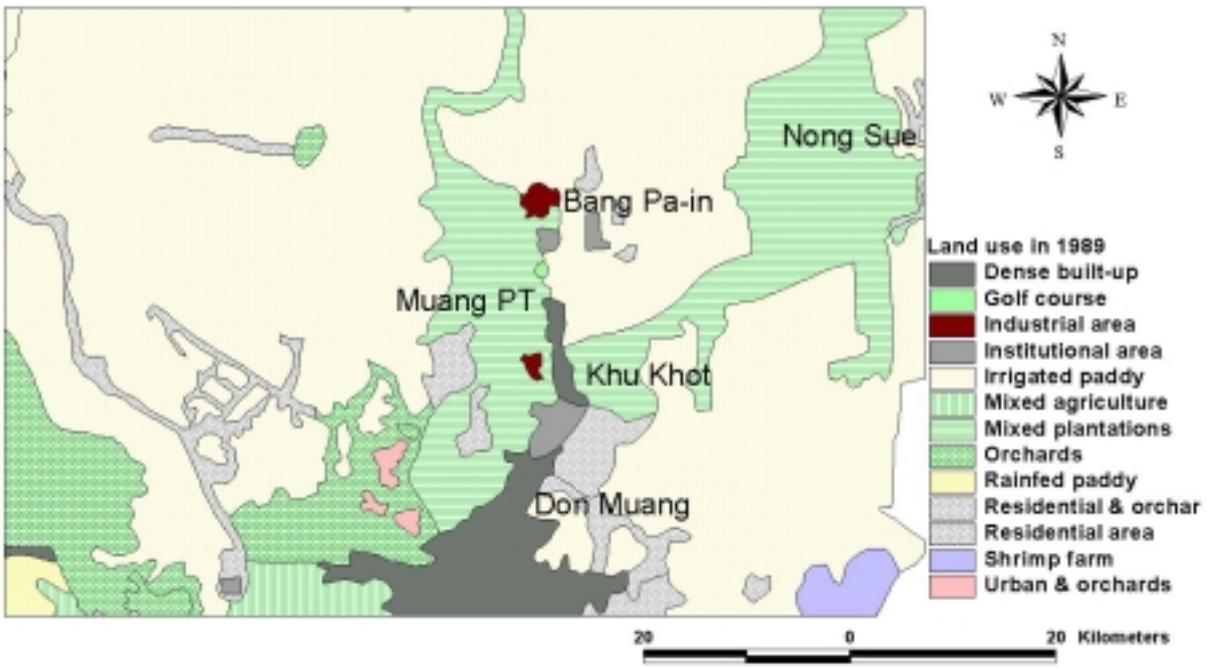

Figure 2 Land use map in the study area in 1988 (Source: *Department of Land Development*, Thailand)

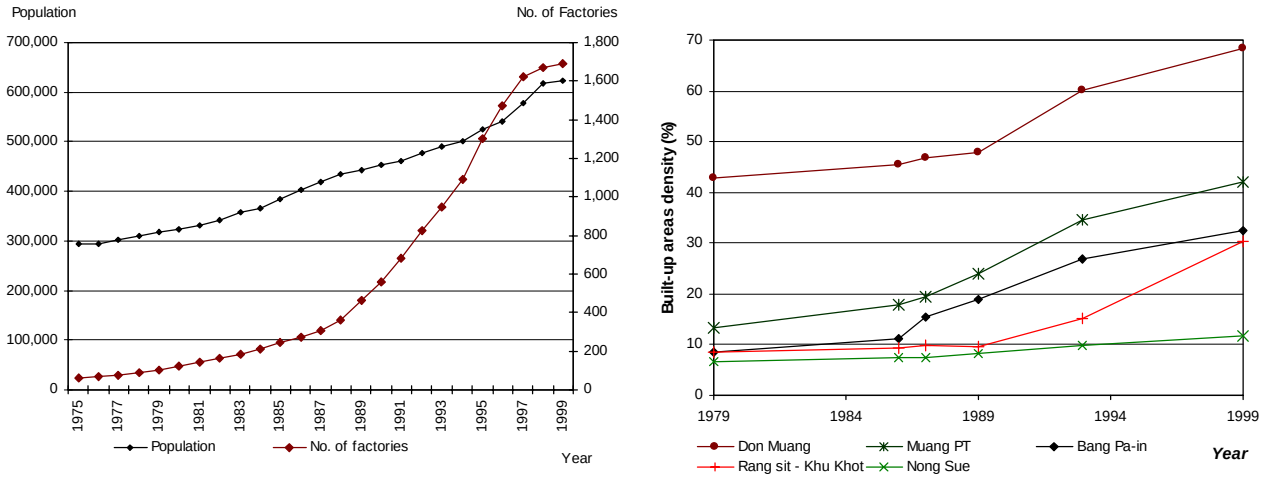

Figure 3 The increase in population and industrial establishments of the Pathum Thani province (a) and the percentages of urbanized areas in various sub-areas of Northern Bangkok (b) during the last two decades.

3. Land Use Change and Sub-urbanization Patterns

Change detection methods were applied to classified images to understand the land-use conversion and to build time-series data for a particular land-use type for the 1979 – 1999 period. The general structure of land-use in the study area has changed significantly for three most important land-use types: paddy land, fruit-tree plantation and built-up areas. During the period of 1989-1999, there were three dominant changes in land-use patterns occurring in the study area as follows:

a. Considerable areas of paddy fields were converted into built-up construction and wasteland-pre-construction areas (13.65 % of paddy land in 1989);

b. Considerable areas of paddy fields are converted into fruit-tree plantation (11.03 % of paddy land in 1989); and

c. Some of plantation farms were abandoned and/or replaced by built-up constructions (28.92 % of plantation areas in 1989).

The spatial patterns of urban development were changing over the years. Along with the continuing urban densification of highly urbanized areas such as Don Muang and Lad Phrao, the urbanization started to expand from the Bangkok Metropolis into the northern suburbs along major roads (Rangsit – Nakhon Nayok, highways No. 306, 346) creating the "ribbon" type of urban development. The main direction of urban expansion during the 1980s was along the so-called Northern Corridor (National Highway No. 1), where most industries and major infrastructure projects located at two major centers Rangsit and Bang Pa-in. The rate of urban expansion was observed of more than 7 percent per year in some neighborhoods of the Northern Corridor. During the last decade, the urban expansion was shifted to the east along Rangsit – Nakhon Nayok highway and to the west through Muang Pathum Thani along highway No. 346 (Tran & Yasuoka, 2000). At the same time, the in-fill development in forms of industrial and associated residential establishment, which has enlarged the urbanized area in perpendicular to the "ribbon" direction, was observed at the Rang Sit – Khu Khot, Bang Pa-in and Muang Pathum Thani sub-areas. In addition, there was some sparse development in forms of individual housing projects and independent industrial/institutional establishments in the agriculture-dominated land of Nong Sue, Lat Lum Kaew districts.

Table 1 The urban development patterns during 1989 – 1999 of five selective sub-areas

Sub-area	**Dominated Land conversion types**	**% of urbanized in 1989**	**% of urbanized in 1999**	**DTI**
Don Muang	"*Urbanized*" to "*Dense Urbanized*"	47.93	68.39	4
Khu Khot	"*Agriculture*" to "*Medium-density Residential*"	9.68	30.24	2

Bang Pa-in	"*Mixed Agriculture*" to "*Industrial/Institutional*"	18.90	32.39	2
Muang Pathum Thani	"*Agriculture/Residential*" to "*Mixed Commercial*"	24.05	41.95	3
Nong Sue	"*Orchards*" to "*Sparse Residential*"	8.32	11.78	1

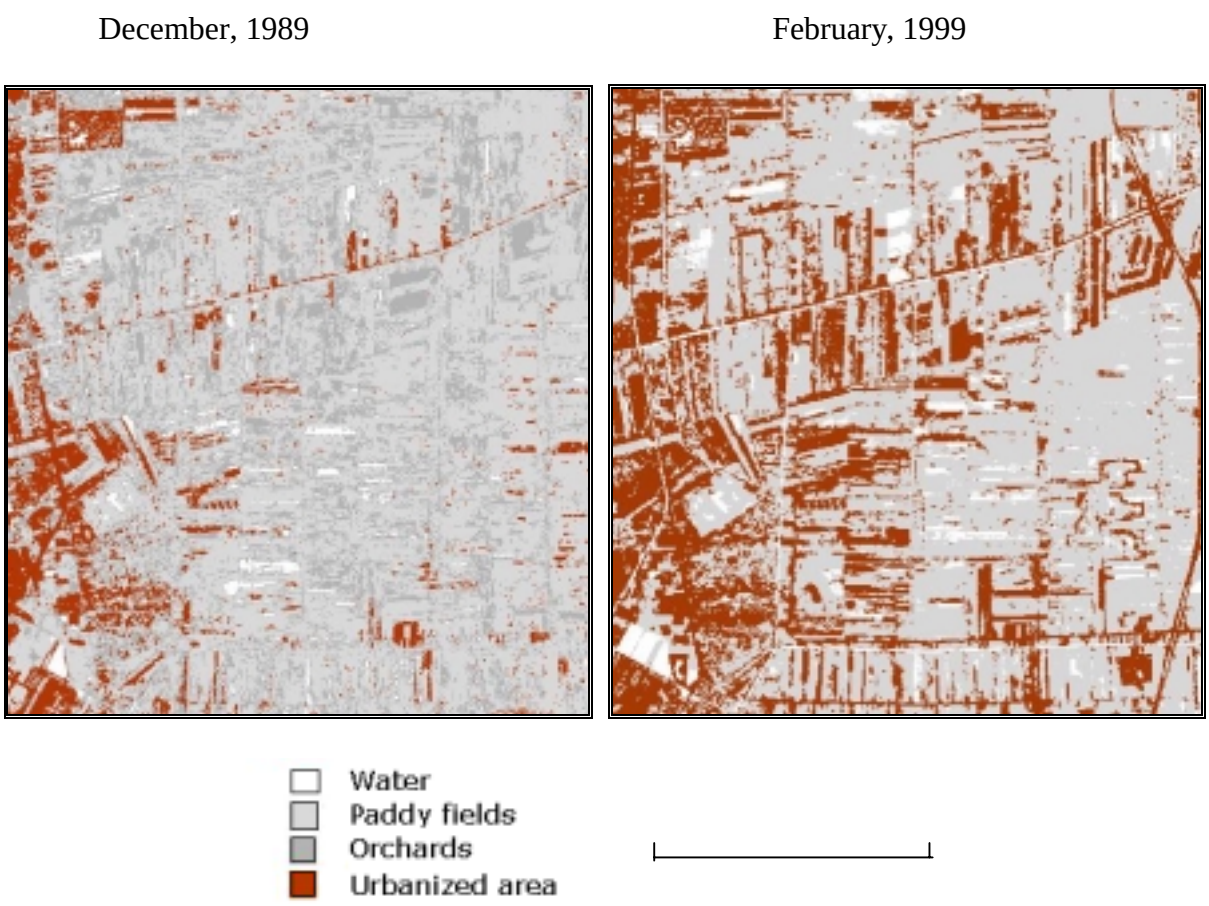

Figure 4 TM derived land cover classifications of the Rang Sit – Khu Khot sub-area between 1989 and 1999.

In the example of Rang Sit – Khu khot sub-area (Figure 4), there were observed extensive commercial complexes at the Rang Sit intersection and extensive residential housing at the center of sub-area as in-fill development during the 1989 – 1999 period. The

percentage of urbanized land in this sub-area was increased from 9.68% in 1989 to 30.24% in 1999, where the new building complexes have replaced the irrigated paddy fields. Based on the type and degree of urban development, we classify the study area into five development classes: unchanged agricultural land; agriculture to sparse urban development (<15% urbanized); agriculture to medium-density (~40% urbanized) urban land, low-density urban to medium-density urban land, medium-density urban to dense urban land (>65% urbanized). These 5 classes are represented as a dummy variable (*Development type Indicator*) with values ranging from 0 to 4 respectively in subsequent analysis. The selective 5 sub-areas namely Don Muang, Khu Khot, Bang Pa-in, Muang Pathum Thani and Nong Sue, representing different urban development patterns in the last decade with characteristics summarized in Table 1. The trends of urbanization over time (1979 – 1999) in these sub-areas were derived using GIS cross tabulation function from classified images and existing land use maps as shown in Figure 3b.

3. Remotely-sensed Biophysical Parameters

3.1 Surface temperatures

The Landsat-TM raw data of 1989 and 1999 were used to extract biophysical surface parameters. Thermal radiances at the original spatial resolution of 120m were converted to at-sensor temperatures via the Planck equation and then to at-surface temperatures based on the following equations developed by the National Aeronautics and Space Agency (NASA):

$$L_{(\lambda)} = L_{\min(\lambda)} + \frac{L_{\max(\lambda)} - L_{\min(\lambda)}}{Q_{cal\max}} Q_{cal} \qquad (1)$$

where

$L_{(\lambda)}$ Spectral radiance received by the sensor for the pixel in question

$L_{\min(\lambda)}$ Minimum detected spectral radiance for the scene (0.1238 $mWcm^{-2}sr^{-1}\mu m^{-1}$)

$L_{\max(\lambda)}$ Maximum detected spectral radiance for the scene (1.56 $mWcm^{-2}sr^{-1}\mu m^{-1}$)

Q_{calmax} Maximum grey level (255)

Q_{cal} Grey level for the analyzed pixel

Once the spectral radiance ($L_{(\lambda)}$) is computed, it is possible to calculate radiant temperature directly by the following equation:

$$T_R = \frac{K_2}{\ln(\frac{K_1}{L_\lambda} + 1)} \quad (2)$$

where

T_R Radiant temperature in Kelvin for the pixel in question

K_1 Calibration constant (60.776 $mWcm^{-2}sr^{-1}\mu m^{-1}$)

K_2 Calibration constant (1260.56 ^0K)

$L_{(\lambda)}$ Spectral radiance for the pixel in question, calculated above in (1)

From the radiant temperature T_R, kinetic temperature T_K, can be calculated using the equation: $T_R = \varepsilon_\lambda^{1/4} T_K$, where ε_λ is the spectral emissivity, assuming to be 0.95 uniformly for the entire terrain/materials in this study.

3.2 Vegetation index - NDVI

NDVI is calculated from visible red (TM Band 3) and near infrared (TM Band 4) reflectances:

$$NDVI = \frac{TM4 - TM3}{TM4 + TM3} \quad (3)$$

The NDVI values were calculated for original 30-m pixel size. They, then, were aggregated as the mean values to 120-m resolution to be compatible with temperature data.

3.3 Universal triangle and land-cover parameters

A normalization procedure was required to compare the changes in biophysical parameters between TM scenes of 1989 and 1999. Without normalization, inter-scene variability in the state of the surface, the phenology of the vegetation and the condition of the atmosphere (e.g., haze, wind speed, humidity) prohibits such a comparison. The water and cloud contaminated pixels, which tend to be localized at negative of NDVI and lower values of T_0, were excluded from the analysis. NDVI was linearly scaled between limits for bare soil ($NDVI_0$) and 100% vegetation cover ($NDVI_s$) (Choudhury *et al.* 1994; Gillies and Carlson, 1995). This linear scaling could also reduce errors in the process of sensor calibration and atmospheric correction. On the 1989 and 1999 images, areas of 100% vegetation cover and bare soil were identified and then, $NDVI_s$ and $NDVI_0$ were selected equaling 0.85 and –0.1 for 1989 and 0.92 and –0.05 for 1999 respectively. Transformation of NDVI to a scaled NDVI (N^*) was accomplished using equation (4):

$$N^* = \frac{NDVI - NDVI_0}{NDVI_s - NDVI_0} \qquad (4)$$

The fractional vegetation cover (Fr) was then calculated as $Fr = N^{*2}$ according to Choudhury *et al.* (1994), Carlson & Ripley (1997).

Temperature values were also scaled between the warmest (T_{max}) and coldest (T_0) surface temperatures corresponding to dry bare soil and wet soil at 100% of vegetation cover. The temperature anchor values were determined by inspection of the NDVI/T_s scatterplots (Owen *et al*., 1998). The observed ambient air temperature (T_a) recorded at the Pathum Thani meteorological observatory at the time of satellite overpass for 1989 (24^0C) and 1999 (22^0C) TM scenes approximately matched the upper corner of the corresponding 'triangle' scatterplots. They were chosen as T_0 for 1989 and 1999 respectively. Consideration was given to the inter-scene variability in terms of precipitation in the few days prior to the scene

acquisition. The warm temperature anchors (T_{max}) were obtained by extrapolation of the warm edge on the scatterplots to the limits of $NDVI_0$, which were 36^0C and 40^0C for 1989 and 1999 respectively. Normalization to a scaled surface temperature was done based on equation (5):

$$T^* = \frac{T_s - T_0}{T_{\max} - T_0} \qquad (5)$$

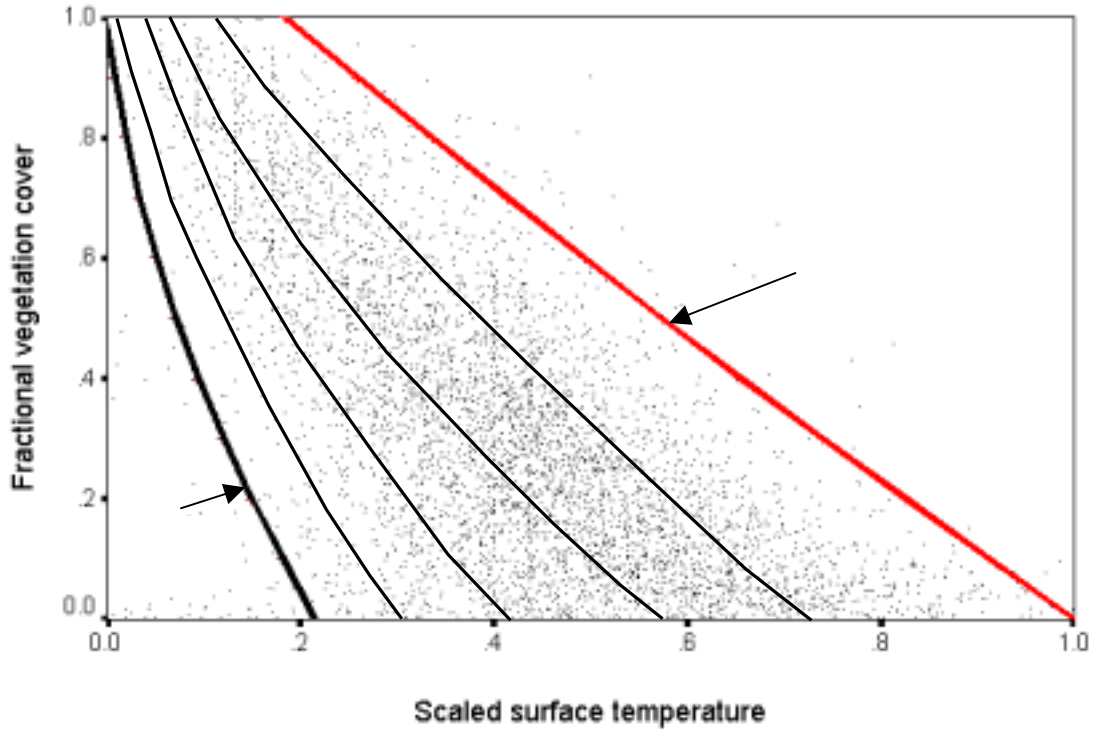

Figure 5 Universal triangle as scaled Fr/T* scatterplot for the February 09, 1999 TM scene resampled to 120-m resolution and overlaid surface moisture availability isolines (M_0 = 0, 0.2, 0.4, 0.6, 0.8, 1) based on the SVAT model output.

The normalized Fr/T* scatterplots were, then, constructed for the 1989 and 1999 TM scenes as the "universal triangle" 120-m pixel envelopes as shown in Figure 5. With the assumptions of unstressed vegetation conditions and zero soil water content along the warm edge of the pixel envelope, the SVAT (soil-vegetation-atmosphere transfer) model of the Penn State University was used to derive fractional vegetation cover (Fr), surface soil water content (M_0) and evapotranspiration fraction (ET/Rn). The observation data recorded from

meteorological stations at Don Muang, Pathum Thani and Ayuthaya were used as input parameters into the model. The SVAT model output in forms of M_0 and *ET/Rn* isopleths were overlaid on the normalized Fr/T* scatterplots using third-order polynomial relations (Figure 5). These 'templates' were then, used to compute the M_0 and *ET/Rn* from *Fr* and *T** for the 1989 and 1999 TM scenes in the study.

4. Rapid Sub-urbanization and Regional Microclimate Changes

To inspect the distribution of surface classes in the Fr/T* nomogram, samples from various land-cover types in the study area were selected and mapped on the scaled scatterplot. Five distinctive groups of pixels as shown in Figure 6 represent dense vegetation, agricultural land, residential area mixed with orchards, bare soil and dense urban area.

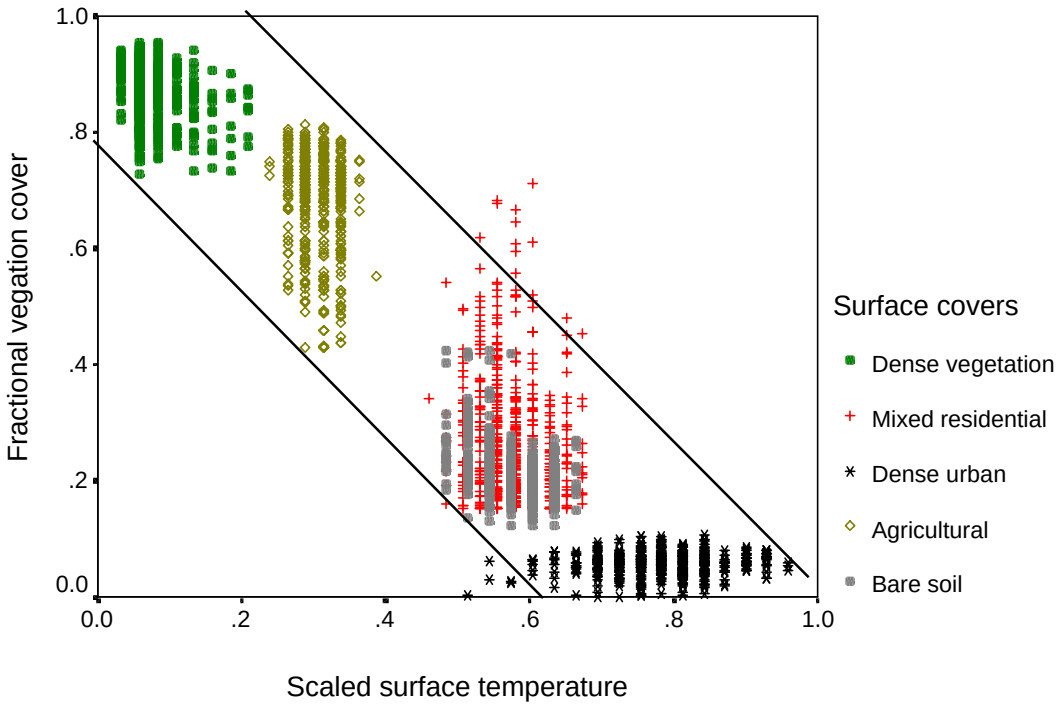

Figure 6 Scatterplot of *Fr* and *T** showing the locations of dense vegetated to dense urbanized surface cover classes.

As shown in figure 6, dense vegetation (predominantly mature fruit-tree plantations) pixels have Fr > 0.7 and cool T* < 0.2, while agricultural land pixels are centered at higher and variable values of T* and considerably lower and variable values of Fr. Dense urbanized pixels, which compose mainly of concrete city blocks, have significant distinctions from other land cover types in terms of surface temperature and vegetation cover (T* > 0.6 and Fr < 0.1). However, suburban residential areas, which normally are surrounded by variable vegetation covers (Fr = 0.1 ÷ 0.7), have large variability in surface temperature T* (0.4 ÷ 0.7). The positions of various land cover types on the scatterplot confirmed the sensitivity of vegetation and surface radiant temperature to urban land use, suggesting variable microclimatic impacts of urbanization. Statistically, it was found a significant negative relationship between percentage of urbanized areas and Fr (*Pearson's r = 0.473* and *p < 0.001*) suggesting a significant loss of vegetation cover in the study area due to rapid urbanization. Surface radiant temperature (T*) was found significantly positively correlated with percentage of urbanized areas (*Pearson's r = 0.491* and *p < 0.0001*). Moreover, the average percentage of urbanized areas in the immediate (3 x 3 pixel) neighborhood was also found to significantly positively correlate with T*, improving the following linear regression relations (*adj.* $R^2 = 0.563$)

$$T^* = 0.406 + 0.00305 * \%\ Urbanized + 0.00333 * \%\ Urbanized\ in\ neighborhood \quad (6)$$

This confirmed that the dense urbanized areas have much higher T* than the sparse urbanized areas surrounded by agricultural fields as the neighborhood development also plays significant part in determining the surface radiant temperature of a pixel. The relationship between M_0 and percentage of urbanized areas, however, was found insignificant. The reasons could be the high intra-pixel surface moisture variability of small-size land parcels in the tropical Thailand.

4.1 Temporal pixel trajectories

To observe changes in the biophysical parameters due to urban development, individual satellite pixels can be located within the 'universal triangle' space over a number of years, thus, depicting a time trajectory (Carlson *et al.*, 2000). As TM pixels are of small size, T* and Fr have considerable large variations creating difficulties in tracing out representative trajectories. The data, therefore, were aggregated from 120-m to 1-km^2 spatial resolution using average values. In the described above 5 sub-areas with different type and degree of urban development, representative 1-km^2 pixels with at least 15% increase in urbanized between 1989 and 1999 were selected. Field observations were conducted to facilitate the selection process and to interpret the resulting trajectories. The control pixel was selected in the west of Muang Pathum Thani area (Figure 2) in the agriculture-dominated area to check for inter-scene variability. Figure 7 shows the trajectories for aggregated TM pixels representing 4 urban development classes (see Section 3). On average, in 1999 the recently developed sub-areas all had significantly higher T*, lower Fr and slightly lower values of M_0 than the mean for the whole area. For the Don Muang sub-area with intensive urban densification from initial highly developed urban area, there was a significant increase in T* (0.4 to 0.77) and significant decrease in M_0 (0.29 to 0.073) between 1989 and 1999. The Khu Khot/Bang Pa-in and Muang PT pixels migrate to warmer (increase in T*) and slight drier (decrease in M_0) positions. It observes a slight difference in between the two trajectories due to the differences in starting positions in the triangle. Field observations confirmed that the Khu Khot pixel (at the center of sub-area in Figure 4) represents the land conversion from wet paddy fields to dense housing complexes and surrounded by wet fallow agricultural fields. The Muang Pathum Thani pixel (at the edge of the Muang Municipality area), on the other hand, represents the land conversion from mixed residential area to the medium-density mixed commercial area. There was much lager decrease in M_0 for Khu Khot pixel (0.24) than

for Muang Pathum Thani pixel (0.07). For the Nong Sue area, the sparse urban development in the irrigated agriculture-dominated areas has increased T* slightly, but did not cause a decrease in M_0. The trajectories show that urbanization was the primary cause of the migration of the pixels in the Fr/T* scatterplot. However, the extent and direction of the path appeared to be governed by other factors such as the pixel's initial location in the triangle and pixel geographical neighborhood. It seems that the later stage of urbanization has caused most regional microclimate changes.

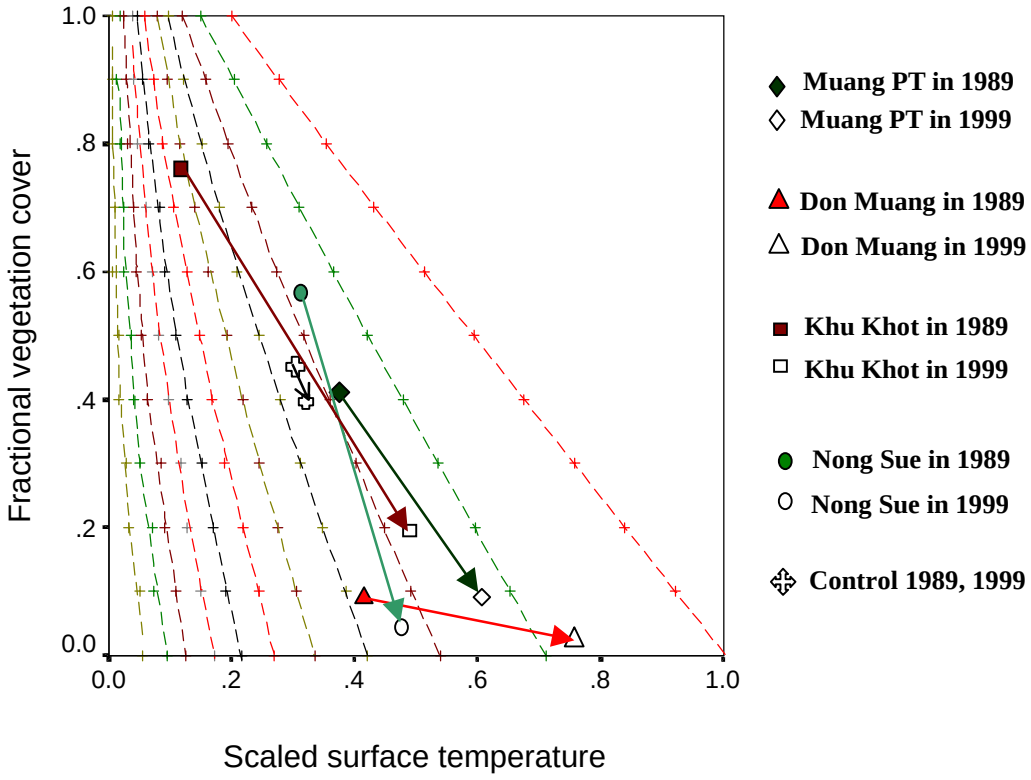

Figure 7 Migration of pixels (aggregated to 1-km^2 from TM pixels) on universal triangle between 1989 and 1999

4.2 Modeling of Microclimatic Changes

Due to atmospheric and surface variability, the absolute surface radiant temperature values derived from satellite images have little meaning in assessing the effects of

urbanization. However, there was a significant increase in standard deviation of T_s in 1999 (2.21^0C) as compared to T_s in 1989 (0.83^0C), indicating there was an increase in average difference of temperature between urban and rural areas. This seems to support the hypothesis that a surface location undergoing urbanization over time will usually experience an increase in T_s resulting from a reduction in both Fr and M_0 (Owen *et al*., 1998). The change in scaled surface temperature (ΔT^*) was then modeled using linear regression to have insights into the effects of urbanization. The exploratory factors were assumed as initial surface conditions (Fr, T^*, M_0 and percentage urbanized in 1989), changes in fractional vegetation cover (ΔFr) and changes in percentage urbanized. As the pixel trajectories within the triangle depend on both the extent and type of development and the land surface's initial conditions (see above), a dummy variable (DTI) was included into the model. The inclusion of neighborhood information in forms of average percentage of urbanized in the immediate 3 x 3 neighborhood has increased the fitness of the model to 0.734. The result of the final stepwise regression model is shown in Table 2, which could be used to predict the future surface temperature for a given development scenario.

Table 2 Linear regression model of changes in surface radiant temperature (ΔT^*) in Northern Bangkok area during 1989-1999

Adj. R^2 = 0.734 Std. Err = 0.0877						
ANOVA		Sum of Squares	df	Mean Square	F	Sig.
	Regression	70.057	7	10.008	1301.401	.000
	Residual	40.274	5237	7.690E-03		
	Total	110.330	5244			

	Unstandardized Coefficients		***Standardized Coefficients***	***t***	***Sig.***
	B	***Std. Error***	***Beta***		

(Constant)	.342	.005		69.828	.000
Scaled surface temperature in 1989 (T*)	-.818	.011	-.660	-77.690	.000
Change in fractional vegetation cover	-.273	.005	-.542	-51.384	.000
Fractional vegetation cover in 1989 (Fr)	-.261	.009	-.301	-28.760	.000
Percentage of urbanized areas in 1989	1.204E-03	.000	.181	15.082	.000
Urbanized area in neighborhood in 1989	1.304E-03	.000	.081	7.990	.000
Development type indicator (DTI)	6.905E-03	.002	.073	7.055	.000
Surface moisture availability in 1989 (M_0)	9.251E-02	.014	.382	6.380	.000
Change in percentage of urbanized areas	2.333E-04	.000	.014	1.617	.106

For the ET fraction (ET/Rn) values calculated by the SVAT model, which show the relationship between sensible heat and latent heat, there was a slight decrease in standard deviation from 0.0759 to 0.0497 between 1989 and 1999, suggesting some effect of urbanization on the change of surface energy fluxes. A stepwise regression model with similar initial exploratory factors was applied to look for significant factors contributing to the changes in ET fraction (ΔET/Rn) with result shown in Table 3.

Two models confirmed the importance of initial surface conditions for a given land parcel in shaping the effects of urbanization on local climatic changes. The surfaces generally become much warmer with less radiant energy being used in evaporative processes due to urbanization if the initial percentage of urbanized increases. The speed of urbanization appeared to affect the change in surface temperature but not the change in evapotransiration fraction. In addition, the vegetation tends to decrease and scaled surface temperature increase with larger amount of initial urban development. As dummy variable (DTI) indicated, the separate low-density housing projects developed within wet agricultural lands did not cause a significant microclimate change. However, at the similar locations, new medium-density

housing complexes could cause an increase in T* up to 30% and a decrease in M_0 up to 20% given all other conditions are equal. At the initially highly developed regions, continuing extensive urbanization has caused most microclimate changes with a decrease in ET/Rn of 11% and an increase in T* of 25%. Similar trends have been noticed by Owen *et al*. (1998) and Carlson *et al*. (2000) for Pennsylvania, USA using regression modeling of sampled developed pixels of low-resolution AVHRR data.

Table 3 Linear regression model of changes in evapotransiration fraction (ΔET/Rn) in Northern Bangkok area during 1989-1999.

Adj R^2 = 0.765 Std. Err = 0.0451					
ANOVA	Sum of Squares	df	Mean Square	F	Sig.
Regression	21.258	5	4.252	2085.962	.000
Residual	10.678	5239	2.038E-03		
Total	31.936	5244			

	Unstandardized Coefficients		***Standardized Coefficients***	***t***	***Sig.***
	B	***Std. Error***	***Beta***		
(Constant)	-.223	.002		-91.046	.000
Scaled surface temperature in 1989 (T*)	.519	.005	.779	95.764	.000
Fractional vegetation cover in 1989 (Fr)	.110	.005	.237	23.833	.000
Percentage of urbanized areas in 1989	-7.453E-04	.000	-.208	-21.709	.000
Urbanized area in neighborhood in 1989	-7.923E-04	.000	-.091	-9.900	.000
Evapotranspiration fraction in 1989 (ET/Rn)	-0.529	.090	-.515	-5.891	.000
Change in fractional vegetation cover	1.438E-02	.003	.053	5.298	.000
Development type indicator (DTI)	-3.3E-03	.002	-.047	-3.42	.001

5. Concluding Remarks

The case study of Northern Bangkok area in this paper demonstrated the capability of satellite remote sensing not only in monitoring the surface development but also in determining useful climate and land surface parameters such as surface temperature, vegetation fraction, ET fraction and surface moisture availability. The study area, where increases in urbanization occurred primarily at the expense of wet agricultural land tended to become warmer and drier between 1989 and 1999. It was found significant changes in these surface climate variables (ΔT^*, $\Delta ET/Rn$), depending on the speed of urbanization as well as the initial percentages of urban coverage and vegetation amount. The most climatic changes were observed where urban expansion continues at the already-developed regions, followed by region of rapid development from wet paddy fields. As the cause of the microclimate changes was determined, it is useful for the urban planners to use remotely sensed land cover parameters to monitor and detect urban-induced environmental changes from the neighborhood to regional scale. Environmentally desirable urban expansion in certain areas rather than others could be argued from findings of such similar studies as we could predict changes in climatic variables given different development scenarios.

The study provided some preliminary results as part of an on-going research at the Institute of Industrial Science, University of Tokyo focusing on “Assessing environmental and disasters risks for sustainable development in Southeast-Asian cities using Remote Sensing / GIS integration”. Continuing works are carrying out to include more factors such as construction materials of city blocks, sub-region’s urbanized structure and stage of urban developments into modeling of microclimate changes. We also plan to use ASTER and ETM+ data for similar studies to derive more accurate surface temperatures at high resolutions (90-m for ASTER and 60-m resolution for ETM+ thermal bands). It is hoped that

the detailed reliable surface parameters can provide deeper insights into the mechanisms of urban-induced surface microclimate changes to use in sustainable development planning.

Acknowledgement

We wish to thank Prof. Carlson T. N. at the Penn State University for providing the executable SVAT model and Mr. Somchai Baimoung at the Meteorological Department of Thailand for providing meteorological observations data to use in this study. We also wish to acknowledge the Japan Society for Promotion of Science (JSPS) for the fellowship given to conduct this research at the Institute of Industrial Science, University of Tokyo, Japan.

Reference

Carlson T.N., Perry E.M. & Schmugge T.J. (1990). Remote estimation of soil moisture availability and fractional vegetation cover for agricultural fields. *Agricultural and Forest Meteorology*, Vol.52, pp.45-69

Carlson T.N. & Arthur S.T. (2000). The impact of land use – land cover changes due to urbanization on surface microclimate and hydrology: a satellite perspective. *Global and Planetary Change*, Vol.25, pp.49-65

Choudhury B.J., Ahmed N.U., Idso S.B., Reginato R.J. & Daughtry C.S.T. (1994). Relation between evaporation coefficients and vegetation indices studied by model simulations. *Remote Sensing of Environment*, Vol.50, pp.1-17

Gillies R.R., Carlson T.N., Cui J., Kustas W.P. & Humes K.S. (1997). A verification of the 'triangle' method for obtaining surface soil water content and energy fluxes from remote measurements of the Normalized Difference Vegetation Index (NDVI) and surface radiant temperature. *International Journal of Remote Sensing*, Vol.18 No.15, pp.3145-3165

Lambin E.F. & Ehrlich D. (1996). The surface temperature-vegetation index space for land cover and land-cover change analysis. *International Journal of Remote Sensing*, Vol.17 No.3, pp.463-487

Nichol J.E. (1996). High-resolution surface temperature patterns related to urban morphology in a tropical city, a satellite-based study. *Journal of Applied Meteorology*, Vol.35, pp.135-146

Owen T.W., Carlson T.N. & Gillies R.R. (1998). An assessment of satellite remotely sensed land cover parameters in quantitatively describing the climatic effect of urbanization. *International Journal of Remote Sensing*, Vol.19 No.9, pp.1663-1681

Ridd M.K. (1995). Exploring a V-I-S (vegetation-impervious surface-soil) model for urban ecosystem analysis through remote sensing comparative anatomy for cities. *International Journal of Remote Sensing*, Vol.16 No.12, pp.2165-2185

Tran H. & Yasuoka Y. (2000). Remote Sensing and GIS to Study the Sub-Urbanization Dynamics: A Case Study in Northern Bangkok, Thailand. *Proceedings of the International Chao Phraya Delta's Conference: Historical Development, Dynamics and Challenges of Thailand's Rice Bowl*, Bangkok, Thailand, Vol.1, pp.111-123.